

УДК 539.126

A NEW EXPERIMENTAL STUDY OF CHARGED $K \rightarrow 3\pi$ DECAYS

*V.Anikeev*¹, *J.Bähr*², *A.Bazilevsky*¹, *A.Bel'kov*³, *G.Bohm*², *S.Denisov*¹,
*A.Durum*¹, *A.Galjaev*¹, *Yu.Gilitsky*¹, *V.Kochetkov*¹, *A.Kozelov*¹,
*V.Kurbakov*¹, *A.Lanyov*³, *A.Lebedev*¹, *Yu.Mikhailov*¹, *A.Moshkin*³,
*V.Onuchin*¹, *V.Shelikhov*¹, *D.Stoyanova*¹

An experimental study was performed of the possibility to use an existing detector — the tagging station of the Tagged Neutrino Facility at IHEP, Serpukhov — for obtaining large statistics data on the decay $K^\pm \rightarrow \pi^0 \pi^0 \pi^\pm$. After giving some motivation for this aim, preliminary results on Dalitz-plot slopes were presented.

The investigation has been performed at the Laboratory of Particle Physics, JINR.

Новое экспериментальное изучение заряженных $K \rightarrow 3\pi$ распадов

В.Аникеев и др.

Проведено экспериментальное изучение возможности использования существующего детектора — станции мечения комплекса меченых нейтрино в ИФВЭ, Серпухов — для получения большой статистики по распаду $K^\pm \rightarrow \pi^0 \pi^0 \pi^\pm$. Приведена физическая мотивация этих исследований, и представлены предварительные результаты по параметрам наклона далиц-плота.

Работа выполнена в Лаборатории сверхвысоких энергий ОИЯИ.

1. Introduction/Motivation

The analysis of nonleptonic kaon decays has been pursued quite successfully already some decades ago. Experiment and theory were found roughly in agreement, the latter using methods like the soft-pion approximation based on current algebra. This general understanding — of course with exceptions, most notably the old question of explaining the $\Delta I = 1/2$ rule — was preserved after the introduction of quarks and some substitutes of QCD in the nonperturbative region: chiral effective Lagrangians, and, with a completely different kind of approximation, lattice QCD.

¹Institute for High Energy Physics, 142284 Protvino, Moscow region, Russia

²Particle Physics Laboratory, Joint Institute for Nuclear Research, 141980 Dubna, Moscow region, Russia

³DESY — Zeuthen, Platanenallee 6, D-15735 Zeuthen, Germany

Meanwhile, the experimental investigations in kaon physics were focused on the questions of direct CP violation and very rare decays connected with flavour-changing neutral currents or even lepton-number violation. A large amount of new data was to be analysed by theory, giving rise to various extensions and refinements of both basic models and calculation methods. Usually, in this more contemporary work, older experimental results, e.g., those on Dalitz-plot slopes in $K \rightarrow 3\pi$ decays, had to be taken for granted, since in quite some cases new large statistics data are not easy to obtain. A remarkable exception is the measurement of the quadratic slope parameters in $K_L^0 \rightarrow 3\pi^0$ decays [1]. The impact of this result on the — older — data of 3π decays in charged and neutral channels has been discussed using only model-independent isospin relations [2], leading to the conclusion that 3π decays of charged kaons also warrant new measurements.

Indeed, in the older investigations of nonleptonic decays, the world averages are dominated by few, sometimes even a single experiment of larger statistics, with errors being dominated by systematic effects, which may explain existing internal discrepancies at 2 st. dev. level.

Of course, it would be difficult to motivate the building of completely new experimental facilities for (re-)measurements of this kind, but, as in the case presented here, the use of existing facilities, eventually with some modifications, is an economic alternative for providing us with valuable data even before the advent of specialized kaon- or phi-factories.

This contribution is mainly concerned with the methodical question how to extract linear and quadratic Dalitz-plot slope parameters from actual experimental data, investigating and correcting the effects of acceptance, resolution and background.

The channel considered here is $K^\pm \rightarrow \pi^0 \pi^0 \pi^\pm$. The Dalitz-plot slopes for $K \rightarrow 3\pi$ decays are defined by the expansion of the squared matrix element in powers of the invariant variables x, y :

$$|T_{K \rightarrow 3\pi}|^2 \sim 1 + gy + hy^2 + kx^2 + \dots,$$

where $y = (s_3 - s_0)/m_{\pi^+}^2$, $x = (s_2 - s_1)/m_{\pi^+}^2$, $s_i = (p_K - p_i)^2$, $s_0 = \frac{1}{3}(s_1 + s_2 + s_3)$, p_K and p_i are the 4-momenta of the kaon and the i -th pion (3 is the index of the «odd» pion).

It will be seen that the definition of slope parameters has as a consequence a strong positive correlation between g and h . This could be avoided by a re-definition of the parameters, introducing orthogonal polynomials in y ; but we prefer to stick to the usual definition, keeping, however, the nondiagonal elements of the covariance matrix for any further use of the results. This is especially important for the analysis of the final state interaction phases with the help of slope parameters g, h, k , where, as has been shown in detail in [2], combinations like $(h + 3k)/g$ are to be studied.

Such phases are of outstanding interest not only as a check of chiral models in higher orders, but also for estimating possible charge asymmetries in $K^\pm \rightarrow 3\pi$ decays, e.g., $\Delta g = (g^+ - g^-)/(g^+ + g^-)$. These estimates [3] critically depend on the values of strong interaction phases. If found experimentally, a value $\Delta g \neq 0$ would be irrefutable evidence for direct CP violation and against the Wolfenstein hypothesis of a superweak interac-

tion [4]. Therefore, the present work may be considered as a preparation — in theoretical and methodical respect — for larger scale efforts focusing on direct CP violation in charged kaon decays.

2. Experimental Set-Up

Almost all detectors used in this experiment have been constructed as a part of the Tagged Neutrino Facility (TNF) at Protvino, where they are used for tagging of neutrinos from charged kaon decays under high rate conditions. The equipment includes:

- beam scintillation and Cherenkov counters for kaon identification;
- beam hodoscopes BH1-BH5 for kaon track measurements and beam adjustment;
- evacuated decay tube;
- 3 scintillation hodoscopes H1-H3 (two planes in each) for tracking of charged secondary particles;
- total absorption electromagnetic spectrometer (TAS) for registration of electrons and gammas.

All detectors listed above were tested during runs at TNF and proved their efficiency. Their configuration (without beam part) is shown in Fig.1.

2.1. Beam Channel. Slow ejected 70 GeV protons are transported from the accelerator to the target using beam channel No.8 [5]. Two dipoles and seven quadrupoles downstream from the target form the beam channel No.23 to select secondaries in the momentum range of 10 to 35 GeV/c ($\Delta p/p$ can be changed from 1.6 % to 8 %) and make a parallel beam (σ_{θ} is about 0.5 mrad). The length of the beam channel No.23 is 60 m, the secondary beam intensity is 10^6 – 10^{10} for positive and 10^5 – 10^9 for negative particles (per cycle, ~ 9 sec).

Beam polarity can easily be changed (this manual procedure takes about half an hour). Another important feature of the beam channel is that it can be operated simultaneously with any internal target experiment, taking only a small part of accelerator intensity.

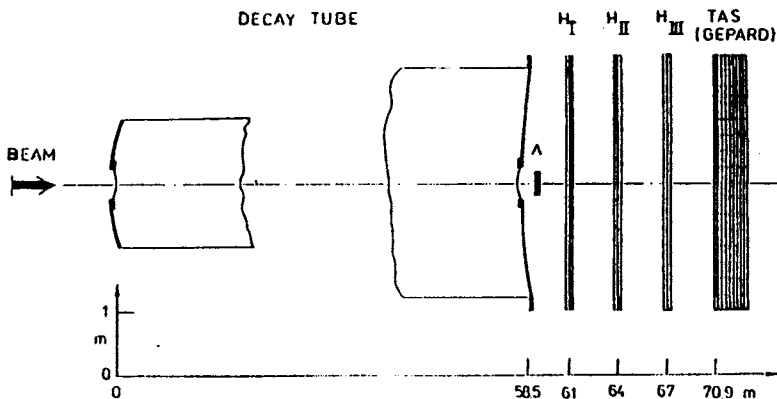


Fig.1. Scheme of experimental set-up

Particle identification is performed with 3 threshold and 2 differential Cherenkov counters. The background level at the kaon peak is less than 1 %. The differential counters are mounted at a moving platform which also allows one to install two magnets for beam deflection during the calibration of TAS with electron beam.

Four scintillation counters are used for triggering, beam intensity measurement and investigation of the time structure of the beam. (A special device allows one to measure the beam intensity up to 10^7 sec^{-1} and to analyse its frequency spectrum up to 100 kHz [6]).

Four beam hodoscopes are used for the determination of the kaon trajectory and beam channel adjustment. Every hodoscope consists of sixteen 15 mm counters in X and sixteen counters in Y (X/Y are horizontal/vertical coordinates in the transverse plane). The counters are overlapped by 1/3 of their width, forming 31 logical elements (of 5 mm width) in each plane. The distance between hodoscopes BH3 and BH4 which are situated downstream of the last magnetic element and are used for tracking is about 10 m. There is also the fifth beam hodoscope BH5, mounted after the decay tube, used only for setting up the beam. It has twice more elements of the same size. Each hodoscope can be moved into/out of the beam by remote control. During data taking, an anticounter of diameter 20 cm placed after the decay tube is used for the selection of decays.

The data considered here are taken with a 35 GeV positive beam of intensity of 10^6-10^7 particles per burst.

2.2. Decay Tube. The 58.5 m decay tube is kept at a pressure of 10^{-4} atm. The end flange is made of 4 mm steel with a smaller beam window of 2 mm aluminium. The beam window itself is carried by a thicker flange of diameter 40 cm bringing 4 cm iron and 4 cm aluminium into our main acceptance region. Such thick flanges complicate the acceptance correction for the experiment, furthermore they degrade the energy resolution of the electromagnetic calorimeter and raise trigger rates from unwanted decays into $\pi^+\pi^0$ and $\pi^0 e \nu$. On the other hand, making the thick flanges obsolete by filling the tube with helium raises some interaction background, which cannot be removed by vertex cuts; M.C. simulation led us to prefer the vacuum solution. Some improvements of the flanges are in preparation.

2.3. Hodoscopes. The hodoscopes of the Tagging Station are of octagonal shape, with size of sensitive area 408×408 cm [7]. Each hodoscope consists of two 512-element planes X and Y . The element width is 1.4 cm, thickness is 1.2 cm, their length varies from 115 to 205 cm. A hole of diameter 20 cm is made in the centre of hodoscopes for passing the beam. The scintillation light is registered by PM's of type FEU-84-3. Further technical details are given in [8,9].

2.4. Electromagnetic Calorimeter (TAS). The total absorption electromagnetic calorimeter consists of 1968 cells [10]. Each cell has 40 alternating scintillators and lead layers with thickness of 5 mm (scintillator) and 3 mm (Pb). The cell size is $76 \times 76 \text{ mm}^2 \times 22$ rad. length; 2 mm thick wave length shifters are used to collect the scintillation light onto PM FEU-84-3. Mylar and black paper sheets between lead and scintillator are used for compensation of the light collection nonuniformity. The HV can be varied individually for every PM for the adjustment of its amplification for the analog sum trigger (see below). The change of HV is performed by potentiometers driven by micromotors which are mounted on the PM base. LEDs are placed near every calorimeter cell. These LEDs are used for the monitoring of the amplification during the HV adjustment.

The calorimeter trigger system analyses the energy deposition in the calorimeter and its topology. It consists of two-stage analog sum circuit, discriminators with software-controlled thresholds and trigger unit TL.

The calorimeter trigger is based on the analog sum signal from 144 channels, forming a field of 1/4 quadrant. This results in 16 such signals from the whole calorimeter. The information about channels above threshold goes via 50 ns delay to the input of the TL unit. The TL unit contains a look-up table which allows one to make a trigger decision in dependence on the number of «fired» trigger channels and their topology.

The calibration of the calorimeter is performed with the help of a 10 GeV/c electron beam swept across the detector surface by two magnets installed upstream of the decay tube. The calibration procedure is similar to those described in [11].

3. Event Selection and Data Evaluation

3.1. Event Selection. For the $K^\pm \rightarrow \pi^\pm \pi^0 \pi^0$ decay mode the on-line data selection was performed by two trigger levels. The first-level trigger is based on signals from beam scintillation and Cherenkov counters and the anticounter at the end of the decay tube. It selects charged kaons decaying inside the decay tube [12]. The second-level trigger is derived from the analog calorimeter signals (see above). It was required to have at least two fields (1/4 quadrants of the calorimeter) with energies above the threshold 1 GeV.

The off-line data selection verifies the on-line cuts, to make easier contact to the M.C. simulation. Furthermore, the following topological criteria were implemented:

- Vertex found: at least one secondary track reconstructed; the distance between primary and secondary track is less than 15 cm; if the primary track has not been reconstructed, the fitted beam axis is taken instead.
- 4 or 5 clusters in calorimeter.
- The following conditions should be fulfilled:

— $N_{\text{track}} = 1$, $N_{\text{cluster}} = 5$, track points to cluster (interacting is assumed);

— $N_{\text{track}} \geq 1$, $N_{\text{cluster}} = 4$, at least one track not pointing to cluster.

For this analysis, we used the data exclusively from the December 94 running period, where we took $\sim 10^7$ triggers with the above-mentioned trigger condition. The running time actually devoted to data taking was ~ 5 days. After processing of the raw data, we found 182200 candidates fulfilling the topological criteria. All events meeting the latter conditions are kept for the further analysis and passed to the kinetical fit, which has to resolve the ambiguities in the ordering of gammas with respect to the two π^0 , to find the energy of the charged pion, to return, among others, the Dalitz variables and to provide a χ^2 probability.

Figure 2 shows the χ^2 probability distribution for the event sample after some additional selection cuts (besides the above-mentioned verification of the trigger conditions some cuts on the vertex position), but before the decisive χ^2 cut. The peak for low probabilities is to be ascribed to (not yet completely identified) background and is removed by

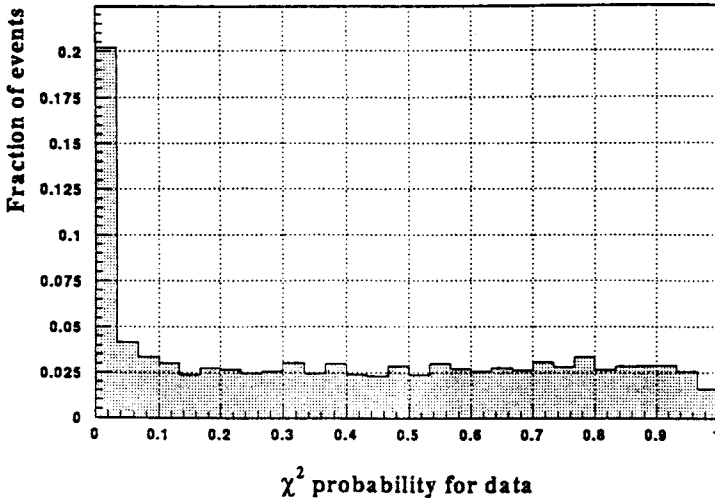


Fig.2. χ^2 -probability distribution for the event sample

the cut at 10 % probability, leaving a final sample of 6748 events. At the present stage, the selection procedure is not optimized for efficiency, but rather for safe background suppression.

3.2. *Estimate of Slope Parameters.* The estimation of slope parameters was done by using a Monte Carlo sample (660000 events generated), where besides the reconstructed Dalitz-plot variables the generated ones are known on an event by event basis. The reconstructed M.C.-Dalitz-plot density was then fitted (by Least Squares and Maximum Likelihood methods) to the observed density by re-weighting the M.C. events with weights, depending on the generated Dalitz-plot variables and the slope parameters searched for (see, e.g., [13] for some general explanations). The most essential condition for a bias-free estimation of slope parameters is the correct simulation of all experimental conditions — acceptance, resolution, and background — by means of the Monte Carlo program. In order to avoid «trivial» mistakes, we used two different M.C. systems and developed also two mainly independent reconstruction chains, allowing us to cross-check both final and intermediate results. In each case, M.C.- and data samples are passed through the same reconstruction chain. Distributions of geometrical and kinematical quantities from both samples have been compared extensively and found in reasonable agreement, with one important exception: the acceptance as a function of the exit points of the charged pions from the decay tube showed some differences in the region of the thick flange at 20 cm radius (see Subsec.2.2).

The straightforward fit of the 2-dimensional Dalitz-plot density revealed indeed a difficulty connected to this mismatch, which we could not yet solve completely. It showed up to be quite unstable with respect to changes of the upper bound for y , tending to produce large values for g and h , being strongly correlated to each other. The reason is to be found in the sensitivity of the acceptance in the large y region, where the charged pions have small emission angles, to details of the exit flange construction of the decay tube. Figure 3 gives

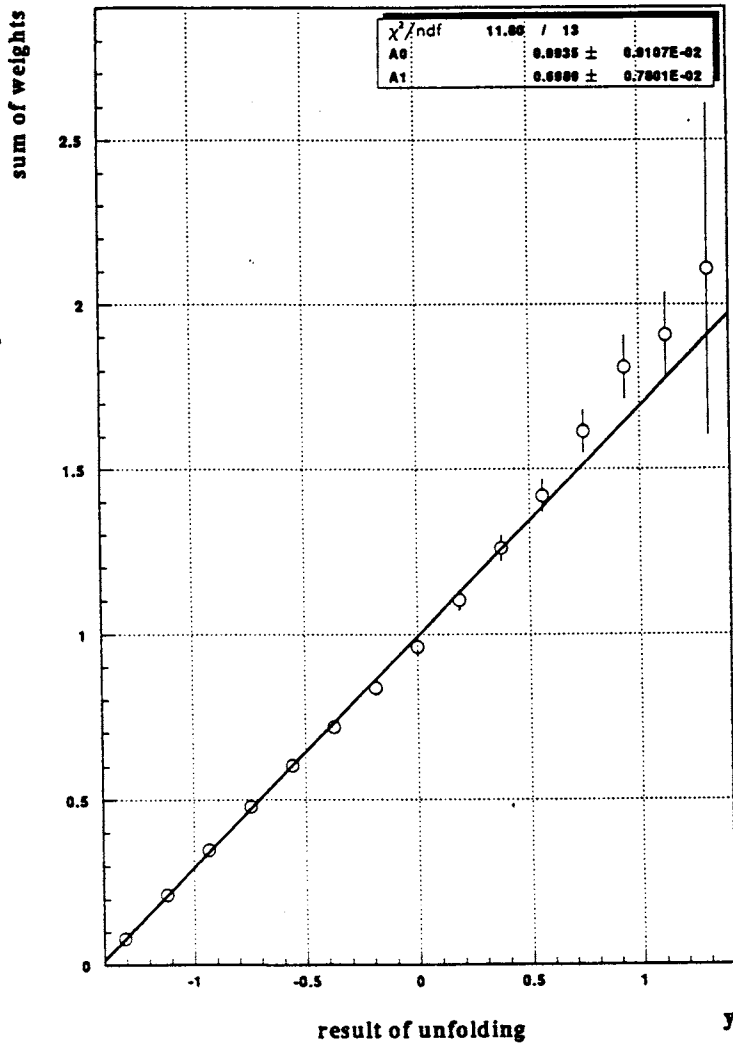


Fig.3. The result of an unfolding procedure for the y distribution

the result of an unfolding procedure for the y distribution, showing that a linear fit is acceptable, at least for lower y, while the uncertain points with large y would drive it to a large quadratic contribution. Stable results were found only after fixing $h=0$ for the slope parameters g and k :

$$g = 0.705 \pm 0.018 \pm 0.020, \quad k = -0.048 \pm 0.006 \pm 0.010$$

(first error, statistical; second, systematical, including error due to M.C. statistics.) The correlation coefficients (g, h) , (g, k) , and (h, k) , obtained from a 3-parameter fit, are, respectively, 0.92, 0.51, and 0.33.

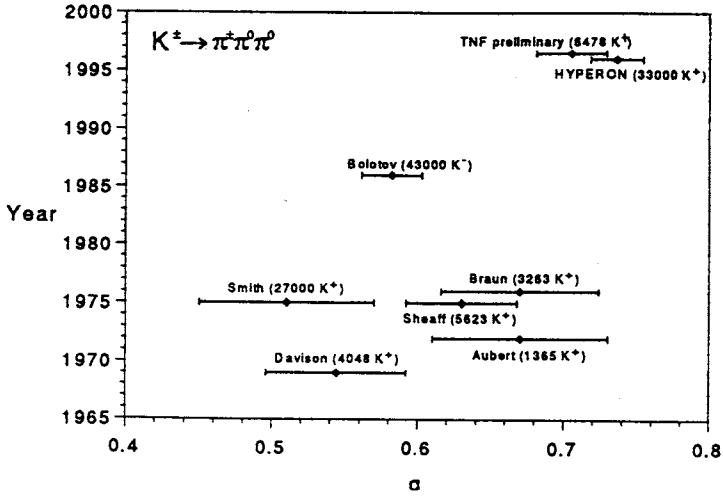


Fig.4. Compilation of measurements of linear slope parameter g : TNF preliminary [16], HYPERON [14], Bolotov et al. [15], Braun et al. [17], Sheaff et al. [18], Smith et al. [19], Aubert et al. [20] and Davison et al. [21]

Our result for the linear slope parameter g is in good agreement with the recent result of HYPERON experiment [14] but about 3σ bigger as compared with the value measured in Protvino at ISTRA experiment by V.Bolotov et al. [15] (see comparison of the experimental data in Fig.4).

The systematic errors were estimated as follows: First, the mismatch between given M.C.- and data distributions was enhanced artificially by re-weighting the M.C. events; then the observed effect on slope parameters was scaled down to the actual residual mismatch between distribution parameters. The error due to M.C. statistics has been derived from comparison with M.C. samples of reduced size. The various contributions are:

- Uncertainty of energy calibration: $\Delta g = 0.006$, $\Delta k = 0.004$;
- Uncertainty of energy resolution: $\Delta g = 0.013$, $\Delta k = 0.008$;
- Uncertainty due to M.C. statistics: $\Delta g = 0.014$, $\Delta k = 0.005$.

The systematic error due to the above-mentioned mismatch concerning the acceptance in the flange region needs further investigation and is therefore not included here.

Some problem is still posed by the possible combinatorial background in the data. We observed some high-frequency structure of the beam, giving rise to spikes in the occupancy of the detectors. The fraction of events suffering from this effect is enhanced by the second level trigger condition derived from the calorimeter signals. So far, this kind of background is not properly taken into account in the simulation. In contrast to background from other kaon decays, which is found negligible after the final selection, we cannot eliminate its possible influence on our results, which therefore, too, are considered as preliminary.

4. Conclusion

In conclusion, we want to emphasize once more, that the results presented here are not final, as several improvements of the data evaluation chain and the M.C. program are in progress; these include, besides the further study of the above-mentioned problems, the application of more refined corrections to the TAS signals, which is possible after extensive *in situ* measurements of shower parameters.

Furthermore, in the next running period it is planned to introduce significant hardware improvements, e.g., a lighter end flange for the decay tube, and to reach a better adjustment of the second level trigger from TAS signals.

It should be clear that a pure enhancement of statistics will hardly improve our knowledge on nonleptonic kaon decays. We need to understand better the systematic errors and to have more different experiments for a critical comparison.

The paper was supported by the Russian Foundation for Basic Research under Grants No. 96-02-16855, No. 96-02-16495.

References

1. Somalwar S.V., Barker A., Briere R.A. et al. — *Phys. Rev. Lett.*, 1992, v.68, p.2580.
2. Bel'kov A.A., Bohm G., Lanyov A.V. et al. — Internal report DESY-Zeuthen 93-05, Zeuthen, 1993.
3. Bel'kov A.A., Bohm G., Lanyov A.V. et al. — *Phys. Lett.*, 1993, v.B300, p.283; *Phys. Part. Nucl.*, 1995, v.26, p.239.
4. Wolfenstein L. — *Phys. Rev. Lett.*, 1964, v.13, p.562.
5. Hagopian M.V. et al. — Preprint IHEP 86-129, Serpukhov, 1986.
6. Kozelov A.V. et al. — Preprint IHEP 92-125, Protvino, 1992.
7. Vasilyev A.V. et al. — Preprint IHEP 92-42, Protvino, 1992.
8. Kotov I.V. et al. — Preprint IHEP 92-41, Protvino, 1992.
9. Denisenko A. A. et al. — *Pribory i Tekhnika Eksperimenta*, 1987, v.1, p.92.
10. Buyanov V.M. et al. — Preprint OHEP 89-45, Serpukhov, 1989.
11. Kulik A.V. et al. — Preprint IHEP 85-17, Serpukhov, 1985.
12. Kozelov A.V. et al. — Preprint IHEP 92-124, Protvino, 1992.
13. Zech G. — Preprint DESY 95-113, 1995.
14. Batusov V.Yu. et al. — In: *Proc. of the 28th Int. Conf. on High Energy Physics*, Editors Z.Ajduuk and A.K.Wroblewski, World Scientific, 1997, p.1200.
15. Bolotov V. et al. — *Sov. Journ. of Nucl. Phys.*, 1986, v.44, p.73.
16. Bel'kov A.A. et al. — In: *Proc. of the 28th Int. Conf. on High Energy Physics*, Editors Z.Ajduuk and A.K.Wroblewski, World Scientific, 1997, p.1204.
17. Braun H. et al. — *Lett. al Nuovo Chim.*, 1976, v.17, p.521.
18. Sheaff M. — *Phys. Rev.*, 1975, v.D12, p.2570.

19. Smith K.M. et al. — Nucl. Phys., 1975, v.B91, p.45.
20. Aubert B. — Nuovo Chim., 1972, v.12A, p.509.
21. Davison D. et al. — Phys. Rev., 1969, v.180, p.1333.